

Numerical Prediction of Minimum Sub-Diffraction-Limit Image Resolved by Silver Surface Plasmon Lenses

Masafumi Fujii

Department of Electric, Electronic and System Engineering, University of Toyama
3190 Gofuku, Toyama, 930-8555 Japan
Tel/Fax: +81 76 445 6762, E-mail: mfujii@eng.u-toyama.ac.jp

Abstract: The minimum possible size of sub-diffraction-limit imaging by the surface plasmon polariton (SPP) induced in thin metal lenses has been analyzed with FDTD method, considering plasmon interference, reflection and transmission of evanescent fields.

OCIS codes: (240.6680) Surface plasmons; (240.6690) Surface waves; (220.3740) Lithography; (160.3918) Metamaterials

1. Introduction

Sub-diffraction-limit imaging capability of thin metal films by means of surface plasmon polarization (SPP) coupled with evanescent waves has been widely investigated theoretically [1] and experimentally [2]. However, it is still unclear with which process and with what material systems, how small images the SPP lenses can resolve. Therefore, in this paper, with the finite-difference time-domain (FDTD) method and analytical Fresnel coefficients, reflection and transmission of evanescent fields in the SPP lensing have been investigated. Moreover, a direct 3D lensing effect of silver films is analyzed precisely, and not only cross sectional fields, but also the realistic 2D images have been demonstrated.

2. Image splitting phenomena of thin metal lens systems

To clarify the effects of the dielectric permittivity and the thickness of the layers to the imaging property, a simple Drude metal of thickness 50 nm is first analyzed, i.e. the relative permittivity of the metal is given by a real function $\epsilon_r = 1 - (\omega_p^2/\omega_o^2)$ with the plasma frequency $\omega_p = 925.5$ THz of silver. The operating frequency ω_o was chosen to be 585.3 THz to give $\epsilon_r = -1.5$, and then two dielectric layer configurations are considered: the one has $\epsilon_r = 2$ for the top photo-resist, -1.5 for the Drude metal, and 1 for the bottom layer below the Drude metal; the other has the opposite order of ϵ_r , i.e. 1 for photo-resist, -1.5 for Drude metal, and 2 for the layer below the Drude metal. Resulting fields are shown in Fig. 1 by energy absorption $W = \int_0^T \sigma |E|^2 dt$ with $\sigma = 1$. Interestingly, these two dielectric layered systems give significantly different field transmission in the layered structure as shown in Fig. 1.

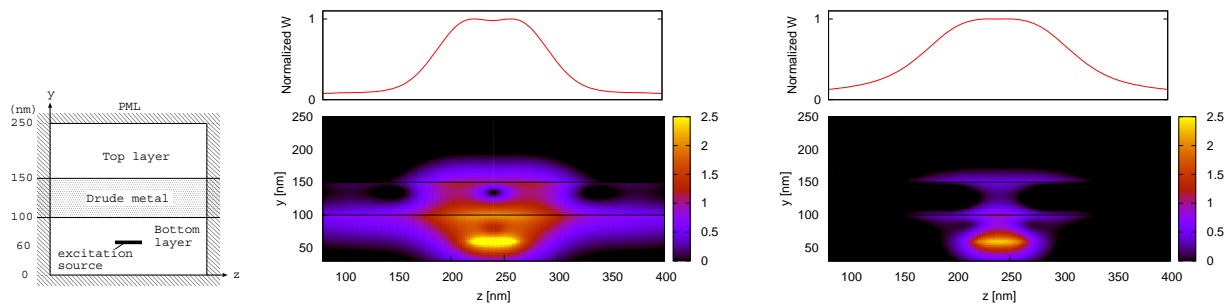


Fig. 1. Field split and focus phenomena in the 3-layered structure. Left: the layered structure under consideration. Center: $\epsilon_r = 2$ for the top, -1.5 for the metal, and 1 for the bottom layers. Right: $\epsilon_r = 1$ for the top, -1.5 for the metal, and 2 for the bottom. The top figures plot normalized W detected at height 155 nm, and the bottom figures are the distribution of W plotted in a logarithmic magnitude color scale. An excitation source of 40 nm in width locates at height 60 nm. The black solid lines indicate the boundaries of the metal layer.

The field splitting and focusing phenomena are found in Fig. 1, which may be explained partly by the differences in the reflection and transmission coefficients calculated by the Fresnel formula. For a p-polarized (or transverse magnetic, TM) light, the Fresnel reflection and the transmission coefficients are calculated using the standard formula and shown in Fig. 2. It is interesting to note that when a light enters from high ϵ_r to low ϵ_r , total reflection occurs at 45 degree incident angle, while for the other case, it is not observed.

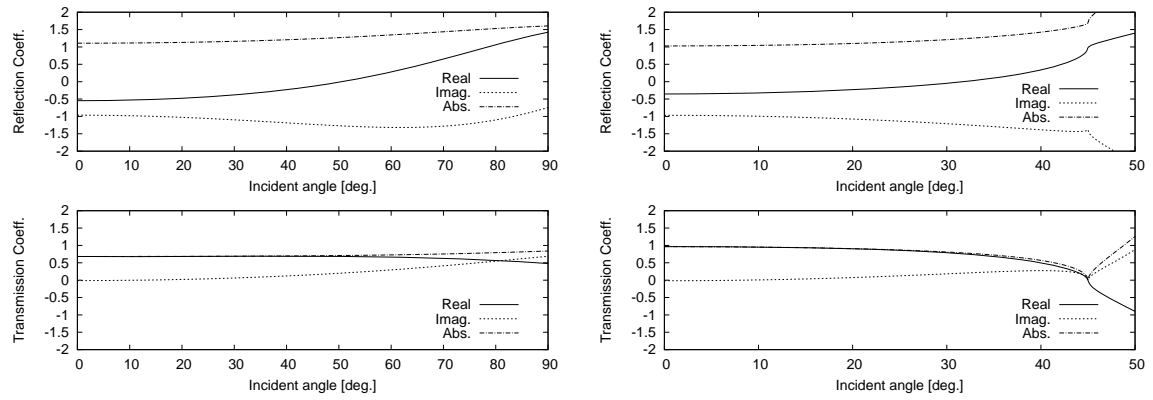


Fig. 2. Overall Fresnel reflection and transmission coefficients R and T , for the layered structures. Left: $\epsilon_r = 2$ for top, -1.5 for the metal, and 1 for bottom. Right: $\epsilon_r = 1$ for top, -1.5 for the metal, and 2 for bottom, and total reflection is observed at 45 deg. Real, imaginary and absolute values are plotted.

3. Sub-diffraction-limit imaging of nano-scale lithography patterns

SPP imaging of round holes and a plus shaped slit has been investigated by taking into consideration precise permittivity of silver and chromium [3]. The layered structure is identical as that of the literature [2]. The mask pattern and the resulting images are shown in Figs. 3 and 4.

For a simple round hole of 40 nm diameter (not shown), the FWHM of the images are 119 nm with a silver layer, and 261 nm without a silver layer. When two holes locate closely, the fields from each holes interfere. In this case the distance between the holes is 167 nm, and the images of the holes are well resolved, while without a silver layer, the images are no longer resolved. The plus shaped slit of Fig.4 has shown a peculiar result; due to the circularly polarized source, the image also rotates slightly. This is due to the interference of the SPP fields on the silver film. In this particular case, the interference worked in such a way that the SPP waves from each section of the slot enhanced. These results show the possibility of producing clearer images for patterns smaller than 100 nm in size.

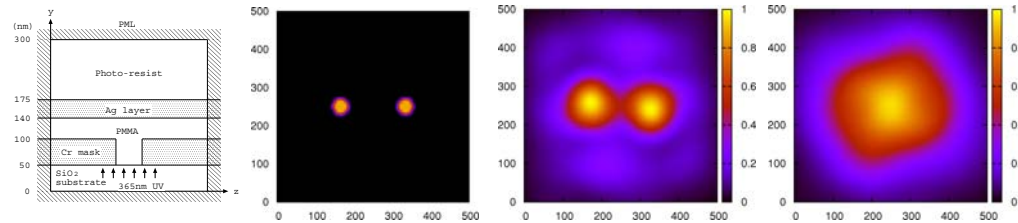


Fig. 3. Layered structure (left), mask pattern (center left) of two 40 nm diameter holes, and the images obtained with (center right) and without (right) a silver thin layer.

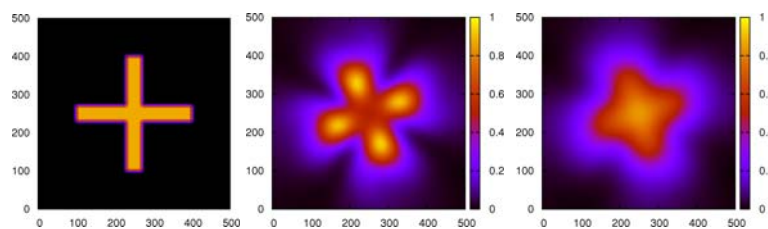


Fig. 4. Mask pattern (left) of 40 nm wide plus shaped slits, and the images obtained with (center) and without (right) a silver thin layer. The layered structure is the same as above figure.

REFERENCES

- [1] J. B. Pendry, "Negative refraction makes a perfect lens", *Phys. Rev. Lett.*, vol. 85, pp. 3966–3969, 2000.
- [2] Nicholas Fang, Hyesog Lee, Cheng Sun, and Xiang Zhang, "Sub-diffraction-limited optical imaging with a silver superlens", *Science*, vol. 308, pp. 534–537, Apr. 2005.
- [3] A. D. Rakić, A. B. Djurišić, J. M. Drazar, and M. L. Majewski, "Optical properties of metallic films for vertical-cavity optoelectronic devices", *Appl. Opt.*, vol. 37, no. 22, pp. 5271–5283, Aug. 1998.